Molecular Therapy
Original Article

Targeting inflammatory macrophages rebuilds therapeutic efficacy of DOT1L inhibition in hepatocellular carcinoma

Yi-Bin Yang,[1,2,3] Cai-Yuan Wu,[1,3] Xu-Yan Wang,[1,3] Jia Deng,[1,2,3] Wen-Jie Cao,[1,3] Yun-Zhi Tang,[1] Chao-Chao Wan,[1] Zhi-Tian Chen,[1] Wan-Yu Zhan,[1] Hong Shan,[2] Dong-Ming Kuang,[1] and Yuan Wei[1]

[1]Guangdong Province Key Laboratory of Pharmaceutical Functional Genes, MOE Key Laboratory of Gene Function and Regulation, School of Life Sciences, and The Fifth Affiliated Hospital, Sun Yat-sen University, Guangzhou 510275, China; [2]Guangdong Provincial Key Laboratory of Biomedical Imaging, Guangdong Provincial Engineering Research Center of Molecular Imaging, and The Fifth Affiliated Hospital, Sun Yat-sen University, Zhuhai 519000, China

Epigenetic reprogramming is a promising therapeutic strategy for aggressive cancers, but its limitations *in vivo* remain unclear. Here, we showed, in detailed studies of data regarding 410 patients with human hepatocellular carcinoma (HCC), that increased histone methyltransferase DOT1L triggered epithelial-mesenchymal transition-mediated metastasis and served as a therapeutic target for human HCC. Unexpectedly, although targeting DOT1L *in vitro* abrogated the invasive potential of hepatoma cells, abrogation of DOT1L signals hardly affected the metastasis of hepatoma *in vivo*. Macrophages, which constitute the major cellular component of the stroma, abrogated the anti-metastatic effect of DOT1L targeting. Mechanistically, NF-κB signal elicited by macrophage inflammatory response operated via a non-epigenetic machinery to eliminate the therapeutic efficacy of DOT1L targeting. Importantly, therapeutic strategy combining DOT1L-targeted therapy with macrophage depletion or NF-κB inhibition *in vivo* effectively and successfully elicited cancer regression. Moreover, we found that the densities of macrophages in HCC determined malignant cell DOT1L-associated clinical outcome of the patients. Our results provide insight into the crosstalk between epigenetic reprogramming and cancer microenvironments and suggest that strategies to influence the functional activities of inflammatory cells may benefit epigenetic reprogramming therapy.

INTRODUCTION

Epigenetic disorder is a decisive feature of tumorigenesis and is implicated in the regulation of intrinsic cancer hallmarks and/or extrinsic immune landscapes.[1–4] The histone methyltransferase DOT1L methylates H3K79 and participates in cell development, cell cycle progression, and DNA damage repair.[5,6] Therapeutic strategies targeting DOT1L activity have been developed in acute myeloid leukemia and have yielded modest clinical effects in phase I trials.[7,8] At present, direct evidence supporting the application prospect of DOT1L targeting in human solid tumors is still lacking. It should be emphasized that the microenvironments of solid tumors are completely different from those of leukemia.[9] A related issue that must be addressed is whether the environmental landscapes of solid tumors control the therapeutic potential of DOT1L-based epigenetic reprogramming strategies and, if so, how they exert that influence.

Macrophages often constitute abundant cellular components in human solid tumors.[10,11] Upon activation, macrophages release a vast diversity of cytokines, growth factors, and inflammatory mediators that may directly influence the behavior of malignant cells.[12] Although activated macrophages may have anti-tumorigenic activity, a high density of macrophages is associated with poor prognosis in most solid tumors.[13] Moreover, recent studies have also revealed that macrophages attenuate the therapeutic efficacy of immune checkpoint blockade therapy.[13–15] Thus, evaluating the composition characteristics of cancer microenvironments will be helpful for the rational design of precise immune-based anti-cancer therapies.

Hepatocellular carcinoma (HCC) usually occurs in inflamed livers where the inflammatory status markedly influences the biological behavior of the malignancy *in situ*.[16,17] In this study, we showed that increased histone methyltransferase DOT1L triggered epithelial-mesenchymal transition (EMT)-mediated metastasis and served

Received 23 February 2022; accepted 28 September 2022;
https://doi.org/10.1016/j.ymthe.2022.09.019.

[3]These authors contributed equally

Correspondence: Hong Shan, Guangdong Provincial Key Laboratory of Biomedical Imaging and Guangdong Provincial Engineering Research Center of Molecular Imaging, The Fifth Affiliated Hospital, Sun Yat-sen University, Zhuhai 519000, China.
E-mail: shanhong@mail.sysu.edu.cn
Correspondence: Dong-Ming Kuang, Guangdong Province Key Laboratory of Pharmaceutical Functional Genes, MOE Key Laboratory of Gene Function and Regulation, School of Life Sciences, Sun Yat-sen University, Guangzhou 510275, China.
E-mail: kdming@mail.sysu.edu.cn
Correspondence: Yuan Wei, Guangdong Province Key Laboratory of Pharmaceutical Functional Genes, MOE Key Laboratory of Gene Function and Regulation, School of Life Sciences, Sun Yat-sen University, Guangzhou 510275, China.
E-mail: weiy58@mail.sysu.edu.cn

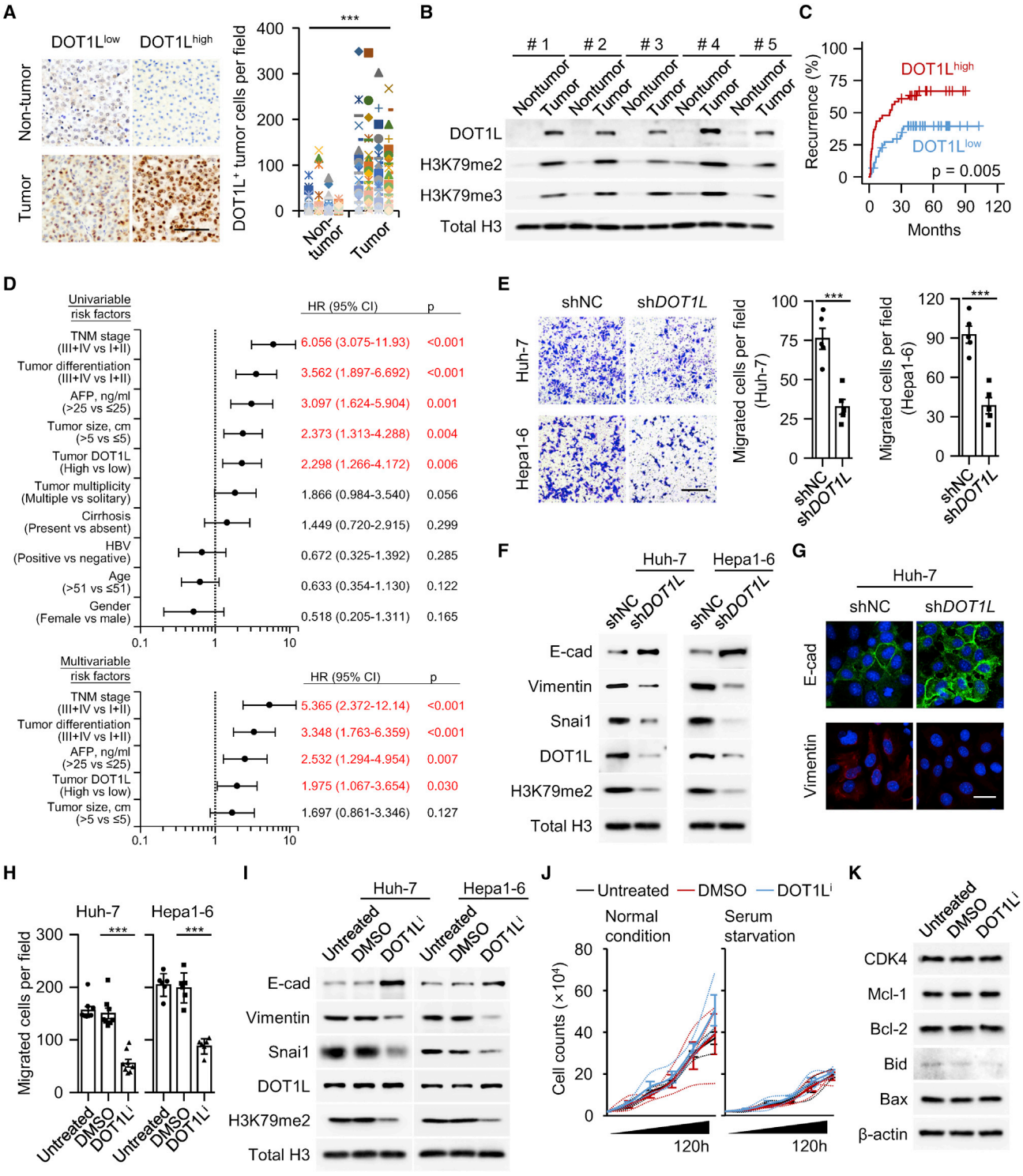

Figure 1. DOT1L serves as a prognostic factor and potential therapeutic target for human HCC

(A) DOT1L distribution in 91 HCC tissues was analyzed by immunohistochemistry. Scale bar represents 100 μm.

(B) DOT1L, H3K79me2, and H3K79me3 expression in HCC tissues was measured by immunoblotting (n = 5).

(legend continued on next page)

as a potential therapeutic target for human HCC. Unexpectedly, macrophages that constitute the major cellular components of HCC abrogated the anti-metastatic effect of DOT1L targeting both *in vitro* and *in vivo*. Mechanistically, NF-κB signal activated by macrophage inflammatory response operated via a non-epigenetic machinery to eliminate the therapeutic efficacy of DOT1L targeting. Importantly, therapeutic strategy combining DOT1L-targeted therapy with macrophage depletion or NF-κB inhibition *in vivo* effectively and successfully elicited cancer regression.

RESULTS

DOT1L operates in EMT-dependent pathway to trigger HCC invasiveness and predicts poor prognosis of patients

To evaluate the potential role of DOT1L signal in tumor pathology, we first investigated the expression and distribution pattern of this protein in human HCC. The expression of DOT1L was visualized by immune-histochemical staining in paraffin-embedded tissues from 91 untreated HCC patients (Table S1). In most HCC samples analyzed, we detected marked expression of DOT1L in the nucleus of malignant cells (78 out of 91 patients, Figure 1A). In contrast, DOT1L signal was hardly detected in non-tumoral region of HCC tissue (Figure 1A). Consistent with this, a significant increase in DOT1L-mediated H3K79 methylation was detected in tumor tissue compared with paired non-tumoral tissue (Figure 1B), indicating that DOT1L signal functioned in tumors of HCC patients. We subsequently divided these patients into two groups according to the median value of nucleated $DOT1L^{+}$ density in intra-tumoral regions. As expected, the density of $DOT1L^{+}$ cells was positively correlated with patients' recurrence (Figure 1C). The $DOT1L^{+}$ cell density was also associated with alpha-fetoprotein levels ($p = 0.005$; Table S2). Univariate and multivariate regression analyses demonstrated that the density of $DOT1L^{+}$ cells was an independent predictor of HCC aggressiveness with significant hazard ratios for predicting clinical outcome (Figure 1D). We came to the same conclusion regarding a validation cohort from The Cancer Genome Atlas (TCGA) RNA-seq data: 80% of the tumor samples showed higher expression of DOT1L than the paired non-tumoral liver samples ($n = 52$; Figure S1A). Increased expression of DOT1L in tumor samples predicted early recurrence of patients ($n = 291$; Figure S1B and Table S1).

We then probed the functions of DOT1L during HCC progression. The expression of DOT1L in human hepatoma Huh-7 cells and mouse Hepa1-6 cells was specifically knocked down by shRNA. We found that such treatment could reduce the motility and invasive potential of malignant cells by 60% (Figures 1E, S1C, and S1D). Consistently, knockdown of DOT1L led to an increase in E-cadherin and a reduction in vimentin in hepatoma cells, suggesting a loss of EMT potential in cells (Figures 1F and 1G). Analogously, Snai1, a transcription factor that triggers EMT process, was also downregulated in DOT1L-knockdown hepatoma cells (Figure 1F). In parallel, we also treated hepatoma cells with a specific DOT1L inhibitor that effectively shed the methyltransferase activity of DOT1L (Figures 1H and 1I). In support of this hypothesis, inhibition of DOT1L activity also impaired the motility of malignant cells to a level similar to that of DOT1L-knockdown cells (Figures 1E–1I). In tumors that highly expressed DOT1L, increases in EMT protein vimentin and Snai1, as well as a reduction in E-cadherin were observed (Figure S1E). Using gene set enrichment analysis (GSEA), we confirmed that genes indicating EMT were selectively enriched in $DOT1L^{high}$ HCC (Figure S1F). Of note, inhibition of DOT1L only marginally affected proliferation of hepatoma cells, even in the case of serum starvation (Figure 1J). Similarly, such treatment could not alter the survival status of the cells exhibiting unchanged Mcl-1, Bcl-2, Bax, and Bid expression (Figure 1K). Hence, DOT1L may mainly contribute to the metastatic potential of malignant cells in HCC.

In vivo microenvironments eliminate therapeutic efficacy of DOT1L targeting

Next, we determined whether targeting DOT1L could inhibit the metastatic potential of liver cancer *in vivo*. Using an autologous murine Hepa1-6 hepatoma model, we detected obvious lung metastasis of cancer cells after 22-day inoculation of Hepa1-6 cells into the liver (Figures 2A–2C). Unexpectedly, inconsistent with the *in vitro* observations, knockdown of DOT1L in Hepa1-6 cells hardly affected lung metastasis in hepatoma-bearing mice (Figure 2B). By analyzing the characteristics of malignant cells isolated from hepatoma-bearing mice, we observed that DOT1L-knockdown Hepa1-6 cells recovered their EMT signature, although these cells still maintained impaired methyltransferase activity (Figures 1F and 2C). Similar results were obtained when we injected DOT1L inhibitor intraperitoneally within the final 12 days of the experiment after the formation of liver cancer in mice (Figures S2A–S2D). Thus, we hypothesized that *in vivo* microenvironments might eliminate therapeutic efficacy of DOT1L targeting. To test this, we exposed DOT1L-knockdown Hepa1-6 cells to conditioned medium from culture of mice tumor-infiltrating

(C and D) Association of $DOT1L^{+}$ tumor cells with patients' recurrence in human HCC. 91 patients were divided into two groups according to the median density of $DOT1L^{+}$ cells in the tumor (C, median, 67): $DOT1L^{low}$ ($n = 45$) and $DOT1L^{high}$ ($n = 46$). Univariate and multivariate regression analyses of factors associated with recurrence were performed (D).

(E–G) DOT1L-knockdown Huh-7 and Hepa1-6 cells were generated by transducing with pLKO-puro lentiviral particles containing shNC or sh*DOT1L* sequences; migration of the cells (E, scale bar represents 100 μm), proteins of EMT genes (F and G, scale bar represents 20 μm), DOT1L, and H3K79me2 expression (F) were determined ($n = 5$).

(H and I) Huh-7 and Hepa1-6 cells were left untreated or were treated with DMSO or an inhibitor against DOT1L ($DOT1L^{i}$); migration of the cells (H), proteins of EMT genes, DOT1L, and H3K79me2 expression (I) were determined ($n = 6$).

(J and K) Huh-7 cells were left untreated or were treated with DMSO or an inhibitor against DOT1L ($DOT1L^{i}$); proliferation of cells under normal condition or serum starvation (2% FBS) was measured (J, $n = 4$). Proteins of survival genes in serum-starvation cells were determined by immunoblotting (K). Results represent three independent experiments. Data represent mean ± SEM. ***$p < 0.001$, Student's t test for (A) and (E), one-way ANOVA followed by Bonferroni's correction for (H).

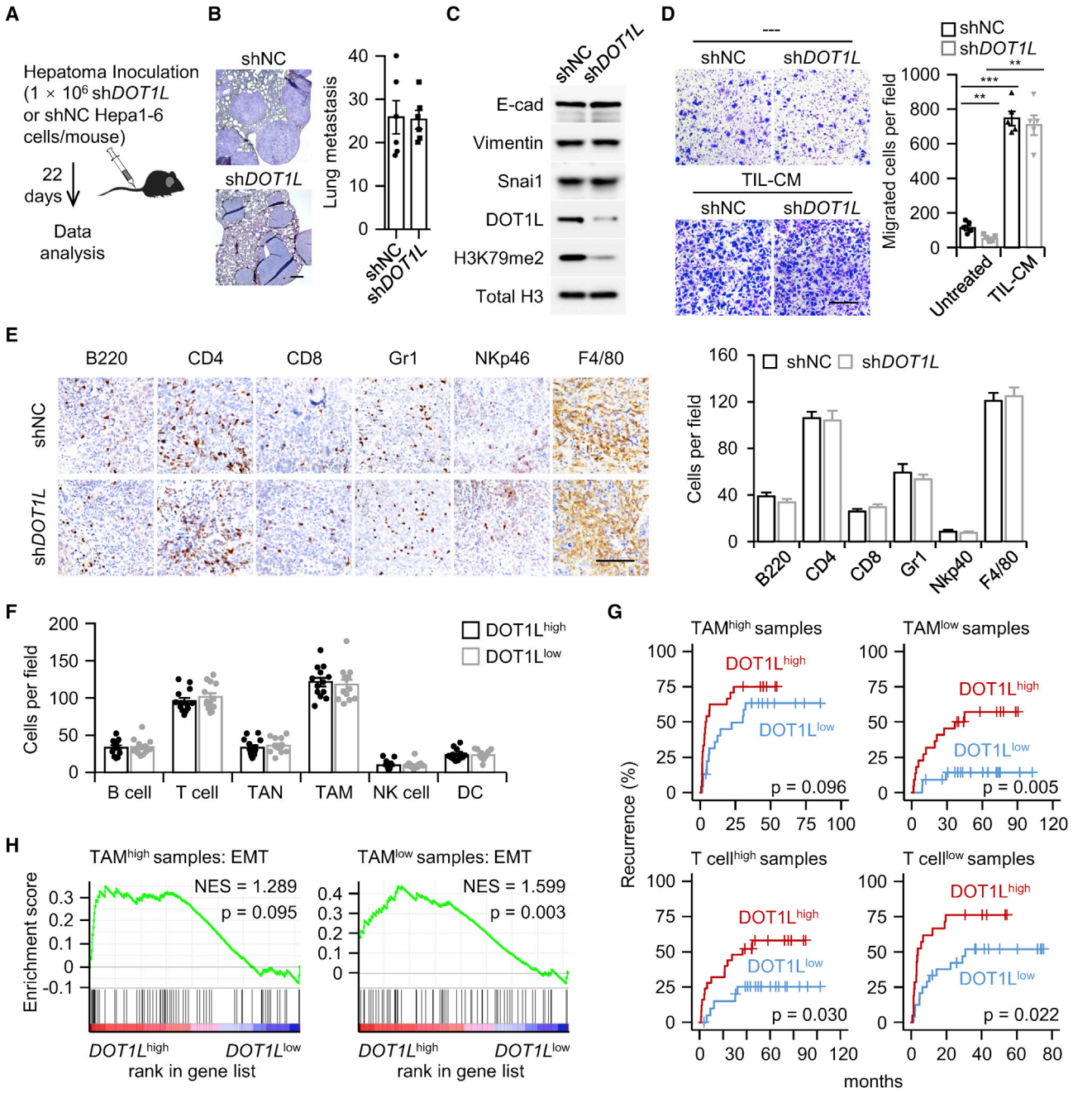

Figure 2. *In vivo* immune microenvironment dismantles therapeutic efficacy of DOT1L targeting

(A–C) Wild-type (shNC) or DOT1L-knockdown (sh*DOT1L*) Hepa1-6 cells were inoculated in liver of the mice for 22 days as described (A). Lung metastasis (B, scale bar represents 250 μm) and proteins of EMT genes, DOT1L, and H3K79me2 (C) in mice tumor tissues were analyzed (n = 6).

(D) shNC or sh*DOT1L* Hepa1-6 cells were left untreated or were treated with conditioned medium from mice tumor-infiltrating leukocytes (TIL-CM); migration of cells was determined (n = 5, scale bar represents 100 μm).

(E) Effect of malignant DOT1L-knockdown on the infiltration of B cells (B220$^+$), T helper cells (CD4$^+$), cytotoxic T cells (CD8$^+$), neutrophils (Gr1$^+$), macrophages (F4/80$^+$), and NK cells (NKp46$^+$) in mouse hepatoma (n = 6, scale bar represents 100 μm).

(F) Human HCC samples were divided into two groups according to the staining results of malignant DOT1L. B cell, T cell, neutrophil (TAN), macrophage (TAM), NK cell, and DC densities in HCC tissues were counted (n = 26).

(legend continued on next page)

leukocytes (TIL-CM) and found that this treatment led to an excessive recovery of cell motility, which was even 10-fold higher than that of wild-type Hepa1-6 cells (Figure 2D). Notably, after exposure to TIL-CM, we could not detect any difference in the motility of wild-type and DOT1L-knockdown Hepa1-6 cells (Figure 2D). Furthermore, we also evaluated whether knockdown of DOT1L in hepatoma cells affected the microenvironment *in vivo*. As shown in Figure 2E, knockdown of DOT1L hardly affected the infiltration of B cells, T cells, neutrophils, NK cells, and macrophages in tumors. In fact, in human HCC samples, there was no difference in the immune cell infiltration pattern between $DOT1L^{high}$ and $DOT1L^{low}$ tissues (Figure 2F). These findings suggest that intrinsic *in vivo* microenvironments determine therapeutic efficacy of DOT1L targeting.

We subsequently evaluated whether *in vivo* microenvironments influenced DOT1L-associated clinical outcome of HCC patients. Considering that macrophages and T cells represent the two most abundant immune cells in HCC tumors (Figure 2F), we stratified patients according to the median values of $DOT1L^{+}$ cell density and either macrophage or T cell density in tumor regions. Interestingly, in patients with low infiltration of macrophages, there is a striking positive association between malignant DOT1L expression and patients' recurrence (Figure 2G and Table S1). In contrast, in patients with high infiltration of macrophages, malignant DOT1L expression is unrelated to the recurrence (Figure 2G and Table S1). Dissimilarly, T cell infiltration hardly affects the prognostic value of DOT1L (Figure 2G and Table S1). Consistent with the above observations, genes related to EMT process were selectively enriched in $DOT1L^{high}$ HCC only in patients with low infiltration of macrophages (Figure 2H). Thus, infiltration pattern of macrophages determines the malignant DOT1L-associated clinical outcome of HCC patients.

Activated macrophages abrogate the anti-metastatic effect of DOT1L targeting

The results described above suggested that macrophages might represent the major factor responsible for abrogating the anti-metastatic effect of DOT1L targeting. In support, exposing DOT1L-knockdown or -inhibited Huh-7 cells to CM from HCC-derived macrophages (TAM-CM), but not those from B cells, T cells, or NK cells, resulted in significantly increased motility and invasive potential of the cells, which also showed signature of EMT (Figures 3A–3F and S3A–S3C). Although CM from tumor-infiltrating neutrophils can also modestly promote migration of the cells (Figure 3B), the neutrophils were rarely detected in intra-tumoral regions of HCC (Figure 2F). As expected, exposure to TAM-CM did not alter DOT1L expression or downstream H3K79 methylation in Huh-7 cells (Figures 3G and 3H). Thus, macrophages reboot malignant aggressiveness and conceal the effect of DOT1L inhibition in an epigenetic independent manner.

Furthermore, we also observed that CM from blood monocytes negligibly affected the motility of DOT1L-knockdown cells (Figure 4A) and therefore analyzed the transcriptional profiles of monocytes/macrophages isolated from HCC tumors and paired blood samples (GEO: GSE140228). We identified 103 genes that were upregulated at least 2-fold in tumor macrophages and annotated these genes using Gene Ontology (GO) (Figure 4B). Among the top 10 enriched GO terms, five pathways related to macrophage activation were intensively enriched (Figure 4B). Consistently, we observed that a large proportion of macrophages isolated from HCC tumor tissue exhibited an $HLA\text{-}DR^{high}CD80^{high}CD86^{high}$ phenotype (Figure 4C). Accordingly, CM from $HLA\text{-}DR^{+}$ activated macrophages, but not that from their $HLA\text{-}DR^{-}$ counterparts, displayed ability to restore the motility of DOT1L-knockdown hepatoma cells (Figures 4D and 4E). We have recently observed that hyaluronan (HA) fragments constitute a common factor produced by several types of human tumors, including hepatoma, to stimulate the activation of macrophages.[11] Therefore, we examined whether hyaluronan fragments endowed macrophages with the function of triggering the motility of DOT1L-knockdown hepatoma cells. Accordingly, using an HA-specific blocking peptide (Pep-1) to attenuate the activation of hepatoma cell-exposed macrophages significantly impaired their ability to retrigger aggressiveness in DOT1L-knockdown hepatoma cells (Figures 4F, 4G, and S4A). In parallel, activated macrophages by exposing to recombinant HA fragments obtained the ability to promote aggressiveness in DOT1L-knockdown cells (Figures 4H, 4I, and S4B).

NF-κB signal links inflammation to DOT1L targeted therapy failure

Given that CM from tumor macrophages counteracted the effect of DOT1L inhibition independently of DOT1L epigenetic activity (Figure 3), we further probed the signals involved in the reinvigoration of DOT1L-deficient hepatoma cells by activated macrophages. As shown in Figure 5A, TAM-CM effectively activated STAT3, PI3K/AKT, MAPKs, and NF-κB pathway in hepatoma cells, and manipulating DOT1L activity hardly affected these processes. Interestingly, blocking the activation of NF-κB signal impaired TAM-CM-induced DOT1L-deficient cancer cell motility (Figures 5B, 5C, and S5A). In contrast, suppressing MAPK, AKT, or STAT3 signals had no effect (Figure 5B).

The results described above demonstrated that activated macrophages played a critical role in recovering the motility of DOT1L-deficient cancer cells (Figure 4). In human HCCs, macrophages showed

(G) 91 HCC patients were divided into four groups according to the median densities of $CD68^{+}$ macrophages and $DOT1L^{+}$ cells, or $CD3^{+}$ T cells and $DOT1L^{+}$ cells in tumors, respectively. Recurrence of the patients was calculated.

(H) Gene set enrichment analysis (GSEA) of EMT signature (GSEA: M1373) in $DOT1L^{high}$ versus $DOT1L^{low}$ counterparts within HCC patients with low or high macrophage infiltration. Results represent three independent experiments. Data represent mean ± SEM. $^{**}p < 0.01$, $^{***}p < 0.001$, one-way ANOVA followed by Bonferroni's correction for (D).

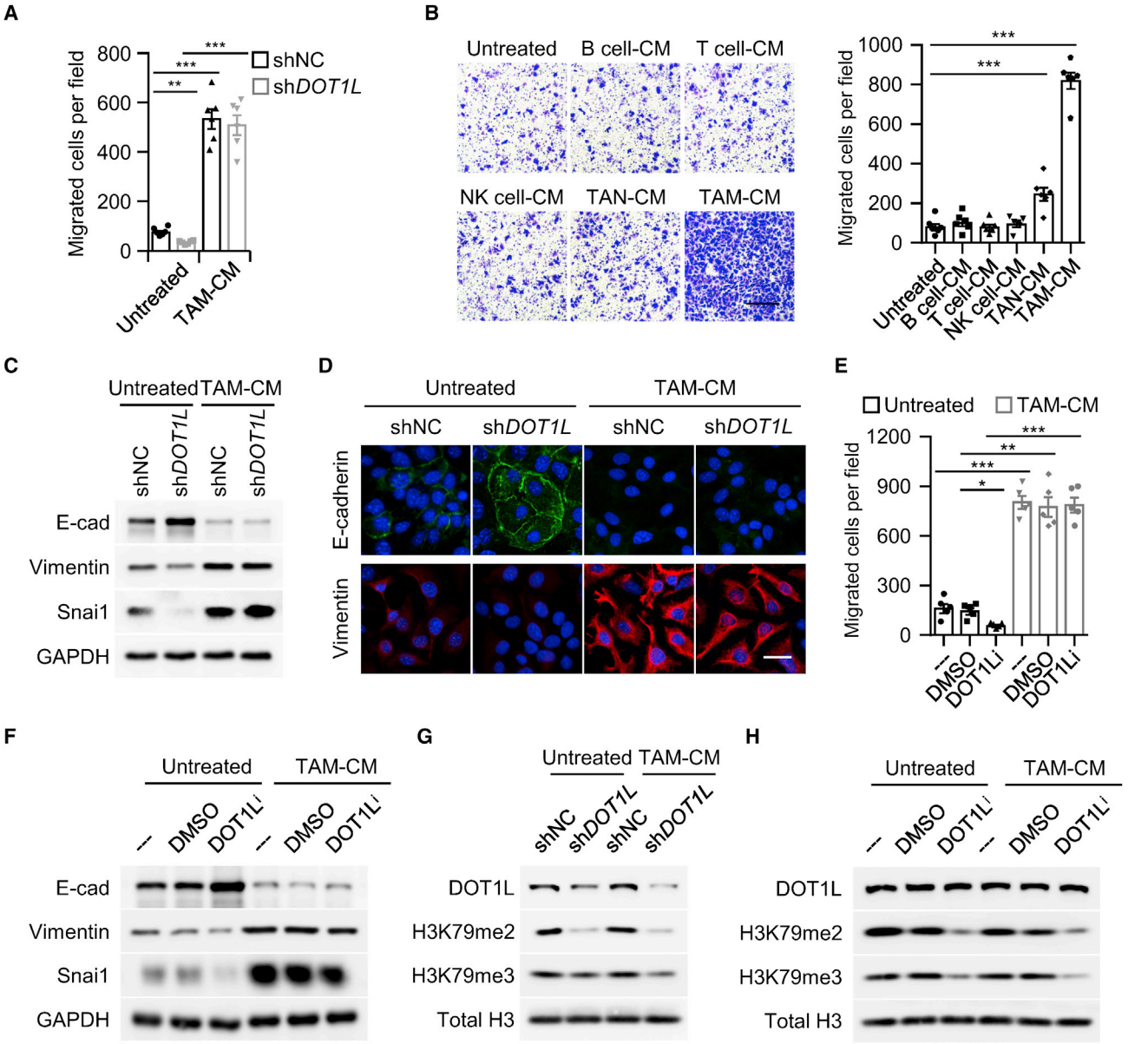

Figure 3. Tumor macrophages abrogate the anti-metastatic effect of DOT1L targeting

(A–D) shNC (A, C, and D) or sh*DOT1L* (A–D) Huh-7 cells were left untreated or were treated with conditioned medium from tumor macrophages (TAM-CM), B cells, T cells, NK cells, or neutrophils as indicated; migration of the cells was determined (A and B, n = 6, scale bar represents 100 μm). Proteins of EMT genes were analyzed by immunoblotting (C) and immunofluorescence (D, scale bar represents 20 μm), respectively.

(E and F) Huh-7 cells were left untreated or were treated with DMSO or an inhibitor against DOT1L in the absence or presence of TAM-CM; migration of the cells (E) and proteins of EMT genes (F) were determined (n = 5).

(G) shNC or sh*DOT1L* Huh-7 cells were left untreated or were treated with TAM-CM, DOT1L, H3K79me2, and H3K79me3 expression was determined (n = 5).

(H) Huh-7 cells were left untreated or were treated with DMSO or an inhibitor against DOT1L in the absence or presence of TAM-CM, DOT1L, H3K79me2, and H3K79me3 expression was also determined (n = 5). Results represent four independent experiments. Data represent mean ± SEM. *p < 0.05, **p < 0.01, ***p < 0.001, one-way ANOVA followed by Bonferroni's correction for (A), (B), and (E).

functional diversity and significantly expressed inflammatory TNF, IL1B, IL12A, IL6, IL10, and TGFB1 (Figures 5D and 5E). We found that neutralizing the activity of TNF-α or IL-1β, which effectively abrogated TAM-CM-elicited NF-κB P65 nuclear translocation, reversed subsequent aggressive hallmarks in DOT1L-deficient hepatoma cells (Figures 5F, 5G, and S5B). Neutralizing other inflammatory cytokines or classical EMT inducer TGF-β hardly affected this process (Figures 5F, 5G, and S5B). Analogously, induction of

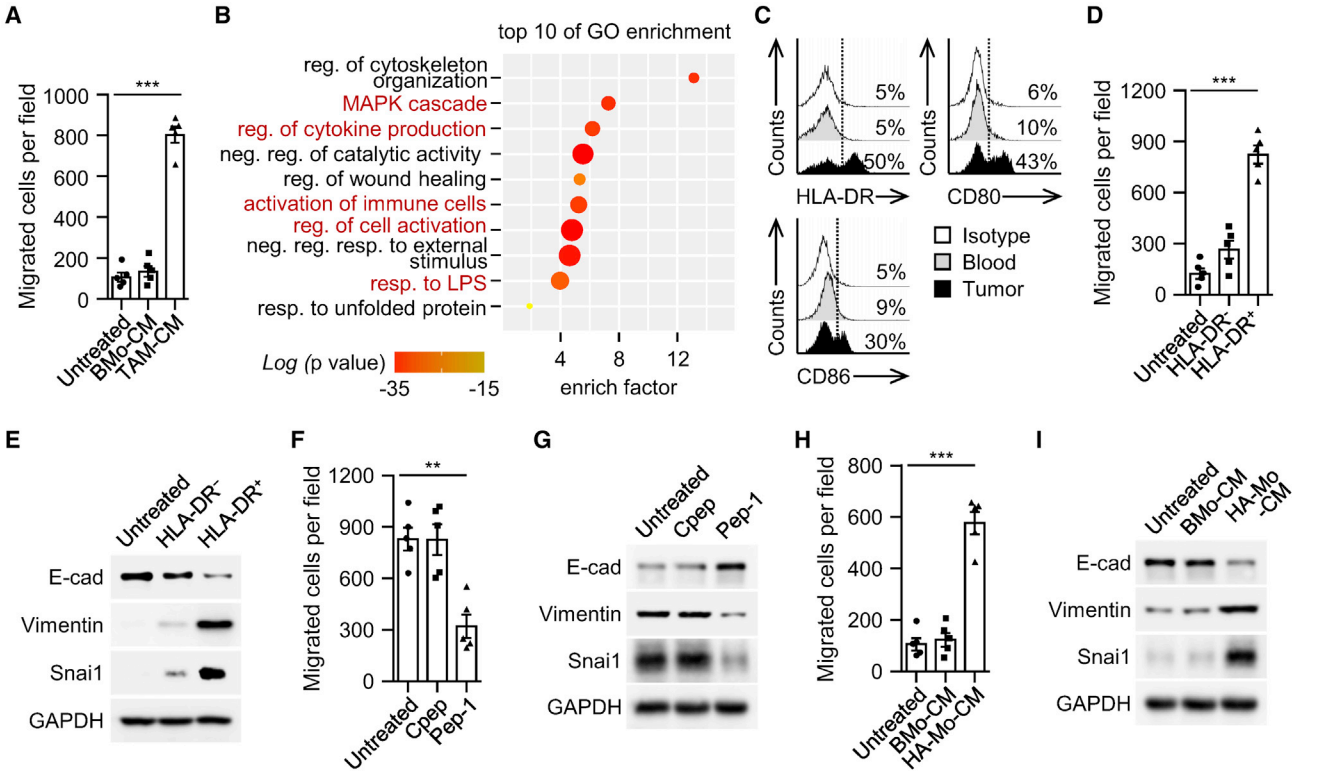

Figure 4. Activated macrophages are more potent in eliminating the effect of DOT1L targeting

(A) sh*DOT1L* Huh-7 cells were left untreated or were treated with conditioned medium from tumor macrophages (TAM-CM) or paired blood monocytes (BMo-CM); migration of the cells was determined (n = 5).

(B) Top 10 biological processes (Gene Ontology terms) enriched in 103 genes significantly upregulated in tumor macrophages compared with blood monocytes in HCC samples (GEO: GSE140228) (FC > 2; p < 0.05).

(C) FACS analysis of HLA-DR, CD80, and CD86 expression on monocytes/macrophages from HCC tumor and paired blood sample (n = 5).

(D and E) sh*DOT1L* Huh-7 cells were left untreated or were treated with conditioned medium from HLA-DR^{-} or HLA-DR^{+} tumor macrophages; migration of the cells (D) and proteins of EMT genes (E) were determined (n = 5).

(F and G) sh*DOT1L* Huh-7 cells were cocultured with blood monocytes in the absence or presence of control peptide (Cpep) or hyaluronan-specific blocking peptide (Pep-1); migration (F) and proteins of EMT genes (G) of sh*DOT1L* Huh-7 cells were determined (n = 5).

(H and I) sh*DOT1L* Huh-7 cells were left untreated or were treated with conditioned medium from untreated (BMo-CM) or hyaluronan-treated (HA-Mo-CM) blood monocytes; migration of the cells (H) and proteins of EMT genes (I) were determined (n = 5). Results represent four independent experiments. Data represent mean ± SEM. ***p < 0.001, one-way ANOVA followed by Bonferroni's correction for (A), (D), (F), and (H).

NF-κB activation in DOT1L-deficient hepatoma cells by exposure to TNF-α or IL-1β contributed in a marked way to generate aggressive malignant cells (Figures 5H, 5I, and S5C). Consistent with the above observation that tumor-derived HA enabled macrophages to transform aggressive hallmarks in DOT1L-deficient hepatoma cells, HA significantly induced TNF-α and IL-1β production in macrophages (Figure S5D). Blocking HA markedly inhibited the production of TNF-α and IL-1β in monocytes exposed to DOT1L-deficient hepatoma cells (Figure S5E). Together, activation of NF-κB signal links inflammatory macrophages to DOT1L targeted therapy failure.

Suppressing macrophage-elicited NF-κB signal augments therapeutic efficacy of DOT1L targeting

To determine whether suppressing macrophage-elicited NF-κB activation could rescue DOT1L-related epigenetic therapeutic efficacy *in vivo*, we initially inoculated wild-type or DOT1L-knockdown Hepa1-6 hepatoma cells into the livers of C57BL/6 mice for 10 days. Thereafter, we used a specific antibody to deplete macrophages in those mice (Figures 6A and S6A). Depleting macrophages partially impaired tumor lung metastasis in both wild-type and DOT1L-knockdown hepatoma-bearing mice (Figure 6B). It should be noted that although DOT1L knockdown marginally affected tumor metastasis in immunocompetent mice, it significantly reduced lung metastasis in macrophage-depleted mice (Figure 6B). These data supported our findings *in vitro* that macrophages elicited resistance of hepatoma cells to therapeutic strategies (Figure 3). We also confirmed the *in vivo* role of macrophages in a therapy model shielding DOT1L function with specific inhibitors (Figures 6C and 6D).

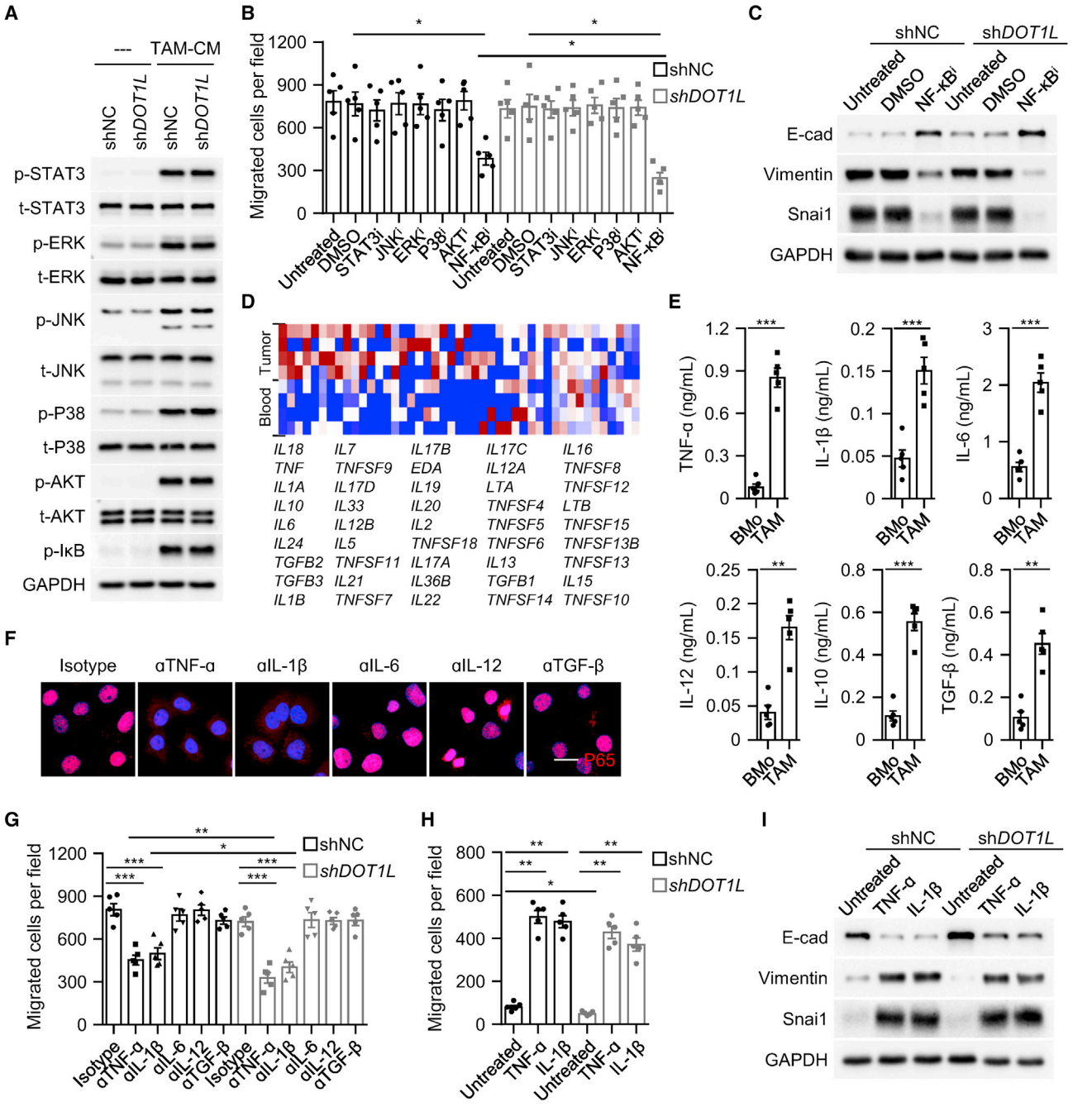

Figure 5. Tumor macrophages abrogate DOT1L inhibition efficacy in an NF-κB dependent manner

(A) shNC or sh*DOT1L* Huh-7 cells were left untreated or were incubated with conditioned medium from tumor macrophages (TAM-CM) for 15 min. Activation of indicated pathways was analyzed by immunoblotting (n = 4).

(B and C) Effects of signaling pathway inhibitors on migration (B) and EMT genes expression (C) of shNC and sh*DOT1L* Huh-7 cells in the presence of TAM-CM (n = 5).

(D) Cytokine expression in tumor macrophages and blood monocytes in HCC samples (GSE140228) was compared (n = 4).

(E) Cytokine production by monocytes/macrophages from HCC blood and tumor was examined by ELISA (n = 5).

(F and G) Effects of cytokine neutralizing on p65 nuclear translocation (F) and cell migration (G) of shNC and sh*DOT1L* (F and G) Huh-7 cells in the presence of TAM-CM (n = 5, scale bar represents 20 μm).

(H and I) shNC and sh*DOT1L* Huh-7 cells were left untreated or were incubated with TNF-α or IL-1β. Migration of cells (H) and EMT marker expression (I) were analyzed (n = 5, scale bar represents 20 μm). Results represent four independent experiments. Data represent mean ± SEM. *p < 0.05, **p < 0.01, ***p < 0.001, one-way ANOVA followed by Bonferroni's correction for (B), (G), and (H); Student's t test for (E).

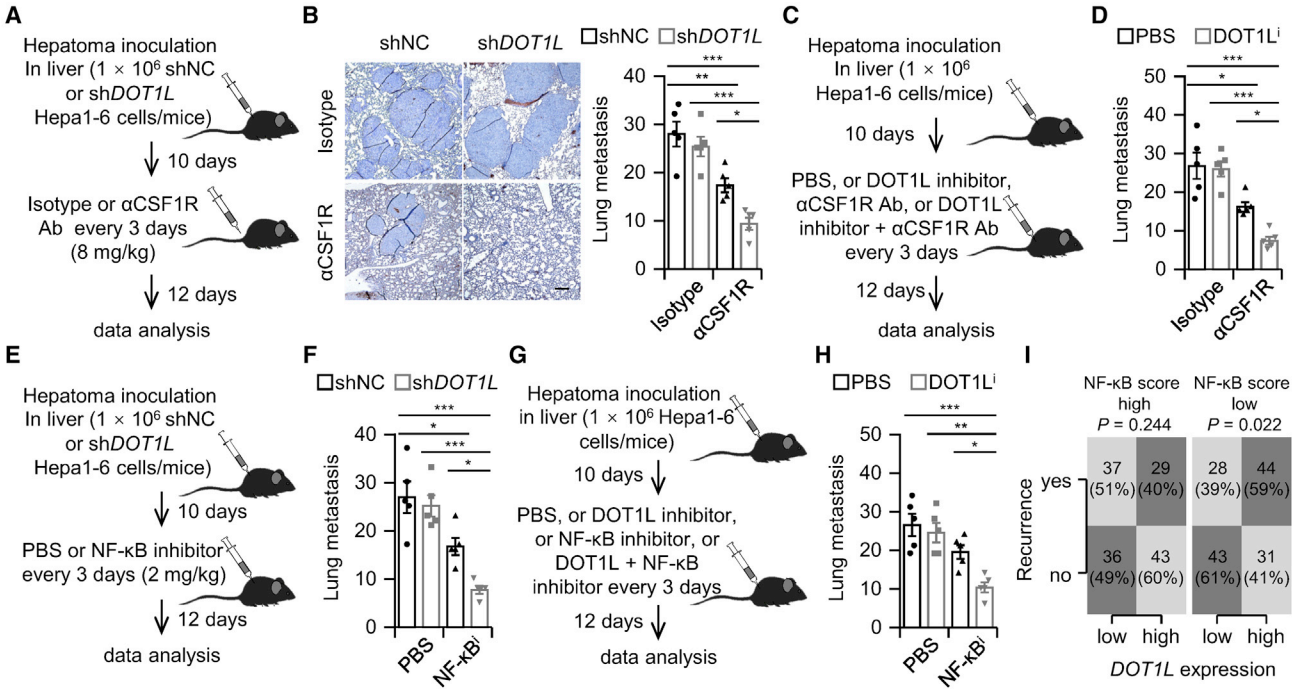

Figure 6. Suppressing macrophage-elicited NF-κB activation augments epigenetic reprogramming efficacy of DOT1L targeting

(A and B) shNC and sh*DOT1L* Hepa1-6 cells were inoculated in mice liver for 10 days. Thereafter, mice were injected with isotype Ab or αCSF1R Ab as described (A). Lung metastasis was analyzed (B, n = 5, scale bar represents 250 μm).

(C and D) Mice bearing Hepa1-6 hepatoma were injected with PBS, DOT1L inhibitor, αCSF1R Ab, or DOT1L inhibitor plus αCSF1R Ab as described (C). Lung metastasis was analyzed (D, n = 5).

(E and F) Mice bearing shNC or sh*DOT1L* Hepa1-6 hepatoma were injected with PBS or NF-κB inhibitor as described (E). Lung metastasis was analyzed (F, n = 5).

(G and H) Mice bearing Hepa1-6 hepatoma were injected with PBS, DOT1L inhibitor, NF-κB inhibitor, or DOT1L inhibitor plus NF-κB inhibitor as described (G). Lung metastasis was analyzed (H, n = 5).

(I) Patients were divided into two groups according to the median value of NF-κB pathway score in 291 HCC samples from TCGA dataset. Associations of tumor DOT1L expression with patients' recurrence in NF-κB score high and NF-κB score low HCC samples were analyzed. p value was calculated by chi-square test. Data represent mean ± SEM. *p < 0.05, **p < 0.01, ***p < 0.001, one-way ANOVA followed by Bonferroni's correction for (B), (D), (F), and (H).

Considering that macrophage-elicited NF-κB signal regulated aggressive features of DOT1L-deficient hepatoma cells (Figure 5), we subsequently inhibited NF-κB signal in Hepa1-6 hepatoma and found that this treatment also partially impaired hepatoma progression *in vivo* (Figures 6E–6H and S6B). In such a model, knockdown of DOT1L in hepatoma cells or injection of DOT1L inhibitor led to marked decrease in lung metastasis (Figures 6E–6H). In line with this, we observed that only in patients with low NF-κB signal signature score could high expression of malignant DOT1L predict early recurrence in HCC patients (Figure 6I). Therefore, our data show that modulating macrophage infiltration or suppressing the NF-κB signal in tumors augments epigenetic reprogramming efficacy of DOT1L targeting.

DISCUSSION

Immune landscapes shape the progression of human cancers.[18,19] In this study, we show that environmental macrophages of DOT1L^{+} tumors control clinical outcome, cancer hallmarks, and therapeutic efficacy in patients.

Epigenetic reprogramming, including histone modifications and DNA methylation, is a newly emerging dimension of tumor intrinsic regulation of gene expression and represents an important tumorigenic mechanism.[2,20,21] DOT1L is to date the only lysine methyltransferase known to mono-, di-, and tri-methylate H3K79 of histone, and this is usually linked to overexpression of genes.[5,6,22] In leukemia, DOT1L has been reported to regulate multiple aggressive biological processes, whose inhibitor was investigated in phase I clinical trials and showed good anti-cancer activity.[7,8] However, whether DOT1L targeting is applicable to the treatment of solid tumors is still unclear. An important difference between solid tumors and leukemia is the microenvironment (TME) formed around solid tumors.[9,23] In our current study, *in vivo* abrogation of DOT1L signals marginally affected tumor aggressiveness, although DOT1L deficiency significantly impaired the motility of malignant cells *in vitro*. In fact, DOT1L-knockdown or -inhibited hepatoma cells regained EMT phenotype after *in vivo* inoculation, indicating the important role of *in vivo* environment in determining the efficacy of DOT1L inhibition. In fact, conditioned medium from tumor-infiltrating leukocytes

significantly recovered the motility of DOT1L-knockdown tumor cells. It is plausible that it is not DOT1L per se, but rather the comprehensive action of intrinsic genetic regulation and environmental factors, that determine tumor aggressiveness and therapeutic efficacy.[24–26] This notion is supported by recent studies showing that multiple potential therapeutic strategies show distinct efficacies in the context of different immune backgrounds.[27–30]

Macrophages represent an important component of tumor microenvironment. Previous studies have shown the pro-tumorigenic role of macrophages in tumor development and treatment.[31,32] Our results indicate that macrophages can also abrogate the anti-cancer potential of DOT1L inhibition. This conclusion is based on the following observations. First, tumor macrophage infiltration determined the malignant cell DOT1L-associated clinical outcome of HCC patients: DOT1L expression predicted worse outcome only in patients with low infiltration of macrophages. Second, coculture with tumor macrophages largely restored the motility of DOT1L-knockdown or -inhibited hepatoma cells without altering DOT1L expression in these cells. Third, depleting macrophages by antibody and shielding macrophage-elicited NF-κB activation by specific inhibitor could significantly enhance the therapeutic efficacy of DOT1L inhibition.

Interestingly, activated macrophages, but not their suppressive counterparts, were more potent in retriggering aggressiveness in DOT1L-knockdown malignant cells. Our results show that innate activation of macrophages elicited by HCC environment altered DOT1L-knockdown malignant cell motility by releasing inflammatory intermediates TNF-α/IL-1β. In breast cancer and colorectal cancer, it has been reported that macrophages exhibit a suppressive phenotype with M2 characteristics.[33–35] Accordingly, in these tumor types, DOT1L inhibition is able to suppress tumor metastasis.[36–39] In fact, enhanced release of the inflammatory cytokines TNF-α, IL-1β, IL-6, and IL-23 by HCC macrophages might also result in Th17-mediated inflammation that in turn stimulates the metastatic and proangiogenic activity of cancer cells by recruiting neutrophils.[40,41] These activated macrophages would thereby repurpose the inflammatory response away from antitumor immunity and toward tissue remodeling and proangiogenic pathways.[40,41]

The macrophage-retriggered motility of DOT1L-knockdown cancer cells observed in our study appears to be independent of epigenetic reprogramming. Snai1 is a well-appreciated master regulated transcription factor for EMT program and subsequent cell motility. It is reported that DOT1L recognizes and facilitates lysine-79 methylation toward histone H3 of the Snai1 promoter, leading to the dissociation of HDAC1 and DNMT1 in the regions and further transcription of the gene.[38] Accordingly, knocking down DOT1L or inhibiting its activity hindered Snai1 expression in hepatoma cell lines. However, exposure to TAM-CM did not compensate for DOT1L expression or the downstream H3K79 methylation process in these cells, although this treatment did rescue the expression of Snai1. In fact, tumor macrophages compensated for Snai1 expression mainly by activating NF-κB signaling. Cytokines that stimulated NF-κB activation could mimic the effect of tumor macrophages to retrigger motility of DOT1L-knockdown cancer cells. Thus DOT1L-mediated H3K79me of the promoter and tumor macrophage-derived inflammatory cytokine-elicited NF-κB activation constitute malignant intrinsic and environmental regulation of Snai1 expression and subsequent tumor aggressiveness. Shielding NF-κB not only abrogated tumor macrophage-elicited recovery of motility in DOT1L-deficient tumor cells *in vitro*, but it also rebuilt the efficacy of DOT1L targeting *in vivo*. In fact, NF-κB is a key player in many important biological processes. Activation of NF-κB signaling has been shown to participate in regulating cell proliferation, survival, migration, invasion, and tumor stemness.[42–45] In addition, NF-κB activation is also involved in malignant PD-L1 expression, which mediates interaction with the local environment.[46] Thus, targeting NF-κB may simultaneously eliminate multiple tumor intrinsic and exogenous hallmarks.

Our results provide important insights into how the immune microenvironment regulates the biological characteristics of DOT1L^{+} cancer cells in human hepatoma. Despite recent success in demonstrating the importance of DOT1L signals during leukemia progression and therapy,[7,8] little is known about its roles and therapeutic potential in solid tumors. In our study, we demonstrated that although DOT1L deficiency significantly impaired malignant cell motility *in vitro*, environmental macrophages can retrigger aggressive hallmarks of the cells and conceal the effect of DOT1L inhibition. In addition to its biological importance, our work may be relevant in clinical management of cancer patients. Our data raise an important clinical question: is DOT1L targeting therapy suitable for cancer patients with a high amount of macrophage infiltration? Alternatively, we suggest that cancer patients can be treated with DOT1L inhibition in combination with strategies targeting the "context" of macrophages and NF-κB signaling. It should be emphasized that tumor macrophages also possess intrinsic anti-tumorigenic properties as antigen-presenting cells. Depleting macrophages not only abolishes their pro-tumorigenic functions, but it also deprives the host of their anti-tumorigenic potential. Analogously, although NF-κB signal contributes to tumor aggressiveness, it is also broadly activated in various immune cells, especially in activated antitumor T cells.[47] Thus, targeting macrophages or NF-κB indeed reshapes the whole immune landscape. Studying the mechanisms that can specifically modulate the functional activities of inflammatory stromal cells or cancer cells would be helpful for developing precise strategies for anti-cancer therapy.[48]

MATERIALS AND METHODS

Patients and specimens

Tissue samples were obtained from 119 patients with pathologically confirmed HCC at the Cancer Center of Sun Yat-sen University (Tables S1 and S3). None of the patients had received anti-cancer therapy before sampling, and those with concurrent autoimmune disease, HIV, or syphilis were excluded. 91 paraffin-embedded tumor samples with complete follow-up data for those who underwent surgical resections between September 2013 and November 2015 were enrolled for analysis of recurrence (cohort 1; Table S1). Paired fresh samples of blood (taken on surgery day) and tumor tissue from 28

HCC patients who underwent surgical resections between August 2019 and September 2021 were used to isolate peripheral and tissue-infiltrating leukocytes (cohort 2; Tables S1 and S3). Clinical stages were classified according to the guidelines of the Union for International Cancer Control. All samples were anonymously coded in accordance with local ethical guidelines (as stipulated by the Declaration of Helsinki). Written informed consent was obtained from the patients, and the protocol was approved by the Institutional Review Board of Sun Yat-sen University (GZR2019-186). 291 HCC samples with complete follow-up data from TCGA dataset were also used for analysis of recurrence (cohort 3; Table S1).

Tumor cell lines

Human hepatoma Huh-7 cells and mouse hepatoma Hepa1-6 cells were obtained from the Cell Bank of the Type Culture Collection of the Chinese Academy of Sciences (Shanghai, China). Experiments were carried out within 6 months after purchase. All cells were tested for mycoplasma contamination using the single-step PCR method and maintained in culture medium composed of Dulbecco modified Eagle medium (DMEM) supplemented with 10% FBS (Gibco).

Immunohistochemistry and immunofluorescence

Paraffin-embedded human HCC or mouse hepatoma samples were cut in 5-μm sections, which were further processed for immunohistochemistry. The sections were incubated with antibodies against human CD3, CD15, CD57, CD68, CD79a, S100, or DOT1L, or antibodies against mouse B220, CD4, CD8, F4/80, Gr1, NKp46, or H3K79me2, and then they were stained in an Envision System (DakoCytomation).

For immunofluorescence analysis of cultured cells, hepatoma Huh-7 cells growing on a cover slide were fixed, permeabilized, and incubated with mouse anti-human E-cadherin or mouse anti-human vimentin followed by incubation with Alex Fluor 488-conjugated anti-mouse IgG, or rabbit anti-human P65 followed by incubation with Alex Fluor 555-conjugated anti-rabbit IgG (Molecular Probes). Nuclei were counterstained with DAPI. Immunofluorescence staining images were visualized by confocal microscopy (LSM880 with Fast airy scan, Carl Zeiss). The antibodies used are listed in Table S4.

Evaluation of immune-histochemical variables

Analysis was performed by two independent observers who were blinded to the clinical outcome. At a low-power field (×100), the tissue sections were screened, and five most representative fields were selected using a Leica DM4 B inverted research microscope. Thereafter, respective areas were measured at ×400 magnification (0.146 mm^2 per field). The numbers of nucleated cells in the tumor regions were then counted manually and expressed as cells per field. There was a significant linear correlation between the counting data of two independent observers ($p = 1.96 \times 10^{-25}$). The average of counts by two investigators was applied in the following analysis to minimize inter-observer variability.

Immunoblotting

Cells from an *ex vivo* or *in vitro* culture system or directly isolated from tissues were washed three times with PBS, and the pellets were re-suspended in lysis buffer for 20 min on ice. After centrifugation at 10,000 *g* for 10 min, the supernatants were dissolved in Laemmli sample buffer and heated at 95°C for 5 min. An equal amount of total protein was separated on 10% SDS-polyacrylamide gel electrophoresis and electrotransferred to polyvinylidene fluoride membranes. The membranes were blocked with 3% BSA, and the presence of indicated protein on the blots was detected with specific antibodies and commercial ECL kit. The antibodies used are listed in Table S5.

Isolation of leukocytes from peripheral blood and tissues

Peripheral mononuclear leukocytes were isolated by Ficoll density gradient centrifugation, and fresh tissue-infiltrating mononuclear leukocytes were obtained as shown in Figure S3A. Fresh HCC biopsy specimens were cut into small pieces (GentleMACS, Miltenyi Biotec) and digested in RPMI 1640 supplemented with 0.05% collagenase IV (Sigma-Aldrich), 0.002% DNase I (Roche), and 20% FBS at 37°C for 30 min. Dissociated cells were filtered through a 150-μm mesh. Thereafter, tissue mononuclear leukocytes were also isolated by Ficoll density gradient centrifugation. The mononuclear leukocytes were harvested and the tumor-infiltrating macrophages, T cells, NK cells, and B cells were further sorted according to CD14, CD3, CD56, or CD19 expression by fluorescence-activated cell sorting (FACS) (Moflo, Beckman Coulter), while neutrophils were purified by magnetic-activated cell sorting (Miltenyi Biotec). In some cases, HLA-DR^+ and HLA-DR^- tumor macrophages were also sorted by FACS.

Preparation of culture medium from tumor leukocytes

Tumor-infiltrating leukocytes were obtained as described above and were washed with medium containing polymyxin B (20 μg/mL; Sigma-Aldrich) to exclude endotoxin contamination. Thereafter, 1×10^6 sorted cells were re-suspended and cultured in 1 mL complete medium (DMEM supplemented with 10% fetal bovine serum) in 24-well cell culture plates. After 24 h, the supernatants were harvested, centrifuged, and stored at −80°C. All specimens were from individuals without concurrent autoimmune disease, HBV, HCV, HIV, or syphilis.

Flow cytometry (FACS)

Monocytes/macrophages from peripheral blood or HCC tissues were stained with fluorochrome-conjugated antibodies according to the manufacturers' instructions. Data were measured by flow cytometer (Gallios, Beckman Coulter) and analyzed using FlowJo software (version 10.0). The fluorochrome-conjugated antibodies used are listed in Table S6.

Construction of viral vectors and sh*DOT1L* cell lines

The candidate sequences for human sh*DOT1L* (sense 5′-CCG GAC CTC TGA ACT TCA GAA TAA ACT CGA GTT TAT TCT GAA GTT CAG AGG TTT TTT G-3′ and antisense 5′-AAT TCA AAA AAC CTC TGA ACT TCA GAA TAA ACT CGA GTT TAT TCT

GAA GTT CAG AGG T-3′), or mouse sh*DOT1L* (sense 5′-CCG GCG CCA ACA CGA GTG TTA TAT TCT CGA GAA TAT AAC ACT CGT GTT GGC GTT TTT G-3′ and antisense 5′-AAT TCA AAA ACG CCA ACA CGA GTG TTA TAT TCT CGA GAA TAT AAC ACT CGT GTT GGC G-3′), or a scrambled sequence for shNC (sense 5′-CCG GCC TAA GGT TAA GTC GCC CTC GCT CGA GCG AGG GCG ACT TAA CCT TAG GTT TTT TG-3′ and antisense 5′-AAT TCA AAA ACC TAA GGT TAA GTC GCC CTC GCT CGA GCG AGG GCG ACT TAA CCT TAG GT-3′) were cloned into pLKO-puro vector (Sigma-Aldrich). Then, the vectors were co-transfected with psPAX2 (Addgene, 12,260) and pVSV-G (Addgene, 138,479) in HEK293T cells using polyethyleneimine (Sigma-Aldrich, 408,727) to generate the lentiviral particles. After 2 days, the lentiviral particles were harvested and enriched through ultracentrifugation. Thereafter, Huh-7 and Hepa1-6 cells were transduced with these shRNA-containing recombinant lentivirus and 8 ug/mL polybrene (Sigma-Aldrich, H9268). Successful transduction was selected using 2 ug/mL puromycin.

Cell migration assay

The migration assay was performed in a 24-well Boyden chamber with an 8 μm polycarbonate membrane (Corning, 3422). Huh-7 or Hepa1-6 cells (3×10^4) in 100 μL of serum-free DMEM were added to the upper compartment of the chamber, and the lower compartment was filled with 600 μL of DMEM containing 10% FBS. After 10 h of incubation, the cells remaining on the upper surface of the membrane were removed. The migrated tumor cells on the lower surface of the membrane were rinsed with PBS and subsequently stained with crystal violet after fixation and then counted under a light microscope (Leica, DM4 B).

Regulation of hepatoma cell migration

shNC and sh*DOT1L* Huh-7 or Hepa1-6 cells were left untreated or were incubated with recombinant TNF-α (20 ng/mL), IL-1β (20 ng/mL), or culture medium from tumor-infiltrating leukocytes, macrophages, HLA-DR$^-$ as well as HLA-DR$^+$ macrophages, T cells, B cells, neutrophils, or NK cells, or *ex vivo* cultured macrophages for 24 h. Migration of the hepatoma cells was determined by transwell. In parallel experiments, Huh-7 or Hepa1-6 cells were left untreated or were treated with DMSO or a specific DOT1L inhibitor (EPZ-5676, 0.1 μM) in the presence or absence of tumor macrophage culture medium. In some cases, shNC or sh*DOT1L* Huh-7 cells were incubated with tumor macrophage culture medium in the presence or absence of neutralizing antibodies against TNF-α (10 μg/mL), IL-1β (10 μg/mL), IL-6 (40 μg/mL), IL-12 (10 μg/mL), or TGF-β (10 μg/mL) (all from R&D Systems). In other set of experiments, shNC or sh*DOT1L* Huh-7 cells were incubated with tumor macrophage culture medium in the presence or absence of specific inhibitors against STAT3 (AG490, 100 μM), JNK (SP 600125, 100 μM), ERK (U0126, 25 μM), P38 (SB 203580, 50 μM), AKT (API2, 100 μM), or NF-κB (BAY 11-7082, 10 μM) signals (Sigma-Aldrich). The recombinant proteins, neutralizing antibodies, and inhibitors used are listed in Table S7.

Ex vivo culture system for monocytes/macrophages

Purified blood monocytes were left untreated or were incubated with intermediate HA fragments (50 μg/mL, Sigma) for 24 h. In some experiments, monocytes were cocultured with hepatoma cells in the presence or absence of a HA-specific blocking peptide (Pep-1, 200 μg/mL, GenePharma) or control peptide (Cpep, 200 μg/mL, GenePharma). The culture medium was collected for further functional assay.

Enzyme-linked immunosorbent assay (ELISA)

Concentrations of the cytokines in the supernatants from *ex vivo* tumor macrophage culture system were detected using ELISA kits according to the manufacturer's instructions (eBioscience, Table S7).

Animal experiments

Wild-type female C57BL/6J mice (3–5 weeks old) were purchased from the Guangdong Medical Laboratory Animal Center (Guangzhou, China). All mice were maintained under specific pathogen-free conditions in the animal facilities of Sun Yat-sen University. All mice were randomly grouped. Mouse Hepa1-6 hepatoma was established as shown in Figures 2A, 6A, 6C, 6E, 6G, and S2A. In brief, 1×10^6 sh*DOT1L* or shNC Hepa1-6 cells in 25 μL Matrigel (3432-005-01, R&D Systems) were injected under the hepatic capsule of the mice. 10 days after hepatoma cell inoculation, the mice were left untreated or were injected intraperitoneally with αCSF1R antibody (8 mg/kg) or NF-κB inhibitor (2 mg/kg) for 12 days at 3-day intervals. 22 days after implantation, tumors were collected and analyzed. In some experiments, wide-type Hepa1-6 cells were implanted into the liver of mice for 10 days; thereafter the mice were left untreated or were injected with αCSF1R or NF-κB inhibitor in the presence or absence of DOT1L inhibitor (EPZ-5676, 5 mg/kg) for 12 days in 3-day intervals. All animal experiments were performed with the approval of the Institutional Animal Care and Use Committee of Sun Yat-sen University.

Cell invasion assay

24-well Boyden chambers with an 8-μm polycarbonate membrane (Corning, 3422) were coated with Matrigel. Briefly, the thawed Matrigel was diluted with a pre-chilled PBS and was added to the upper surface of the membrane before the chamber was placed in a 37°C incubator for 1 h. Thereafter, 4×10^4 Huh-7 cells or 6×10^4 Hepa1-6 cells were plated in the upper chamber and were allowed to invade for 10 h into the lower chamber containing 600 μL of DMEM with 10% FBS. The cells remaining on the upper surface of the membrane were removed. The invaded tumor cells on the lower surface of the membrane were rinsed with PBS and were then fixed and stained with crystal violet for counting (Leica, DM4B).

Statistical analysis

Results are expressed as mean ± SEM. All data were analyzed using two-tailed tests unless otherwise specified. For data normally distributed, we applied the Student's t test; and the non-parametric exact Wilcoxon signed-rank test was used to compare data not normally distributed. For multiple comparisons, an analysis of variance

followed by Bonferroni's correction was applied. All statistical tests were performed with GraphPad Prism (v.6) software. Cumulative survival time was calculated by the Kaplan-Meier method, and survival was measured in months from resection to recurrence or the last review. The log rank test was applied to compare the groups. Univariate and multivariate analysis of prognostic factors for recurrence was performed using the Cox proportional hazards model. $p < 0.05$ was considered statistically significant. All data acquired from animal models were used in analyses.

Data availability

The data that support the findings of this study are included within the article and its supporting information.

SUPPLEMENTAL INFORMATION

Supplemental information can be found online at https://doi.org/10.1016/j.ymthe.2022.09.019.

ACKNOWLEDGMENTS

This work was supported by project grants from the National Natural Science Foundation of China (31830025 to D.-M.K., 81901585 to Y.W., 82025016 to D.-M.K., 82271773 to Y.W., 32200740 to X.-Y.W.) and the Fundamental Research Funds for the Central Universities (22lgqb29 to Y.W.).

AUTHOR CONTRIBUTIONS

Y.-B.Y., C.-Y.W., X.-Y.W., J.D., W.-J.C., Y.-Z.T., C.-C.W., Z.-T.C., and W.-Y.Z. acquired experimental data. H.S. provided administrative, technical, and material support. D.-M.K. and Y.W. conceptualized the study, designed the experiments, and wrote the manuscript.

DECLARATION OF INTERESTS

The authors disclose no conflicts.

REFERENCES

1. Hanahan, D. (2022). Hallmarks of Cancer: New Dimensions. Cancer Discov. *12*, 31–46.
2. Timp, W., and Feinberg, A.P. (2013). Cancer as a dysregulated epigenome allowing cellular growth advantage at the expense of the host. Nat. Rev. Cancer *13*, 497–510.
3. Nishida, J., Momoi, Y., Miyakuni, K., Tamura, Y., Takahashi, K., Koinuma, D., Miyazono, K., and Ehata, S. (2020). Epigenetic remodeling shapes inflammatory renal cancer and neutrophil-dependent metastasis. Nat. Cell Biol. *22*, 465–475.
4. Kim, H., Kim, H., Feng, Y., Li, Y., Tamiya, H., Tocci, S., and Ronai, Z.A. (2020). PRMT5 control of cGAS/STING and NLRC5 pathways defines melanoma response to antitumor immunity. Sci. Transl. Med. *12*, eaaz5683.
5. Nassa, G., Salvati, A., Tarallo, R., Gigantino, V., Alexandrova, E., Memoli, D., Sellitto, A., Rizzo, F., Malanga, D., Mirante, T., et al. (2019). Inhibition of histone methyltransferase DOT1L silences ERα gene and blocks proliferation of antiestrogen-resistant breast cancer cells. Sci. Adv. *5*, eaav5590.
6. Wood, K., Tellier, M., and Murphy, S. (2018). DOT1L and H3K79 methylation in transcription and Genomic stability. Biomolecules *8*, 11.
7. Jones, P.A., Ohtani, H., Chakravarthy, A., and De Carvalho, D.D. (2019). Epigenetic therapy in immune-oncology. Nat. Rev. Cancer *19*, 151–161.
8. Stein, E.M., Garcia-Manero, G., Rizzieri, D.A., Tibes, R., Berdeja, J.G., Savona, M.R., Jongen-Lavrenic, M., Altman, J.K., Thomson, B., Blakemore, S.J., et al. (2018). The DOT1L inhibitor pinometostat reduces H3K79 methylation and has modest clinical activity in adult acute leukemia. Blood *131*, 2661–2669.
9. Hou, A.J., Chen, L.C., and Chen, Y.Y. (2021). Navigating CAR-T cells through the solid-tumour microenvironment. Nat. Rev. Drug Discov. *20*, 531–550.
10. Nakamura, K., and Smyth, M.J. (2020). Myeloid immunosuppression and immune checkpoints in the tumor microenvironment. Cell. Mol. Immunol. *17*, 1–12.
11. Kuang, D.M., Wu, Y., Chen, N., Cheng, J., Zhuang, S.M., and Zheng, L. (2007). Tumor-derived hyaluronan induces formation of immunosuppressive macrophages through transient early activation of monocytes. Blood *110*, 587–595.
12. Locati, M., Curtale, G., and Mantovani, A. (2020). Diversity, mechanisms, and significance of macrophage Plasticity. Annu. Rev. Pathol. *15*, 123–147.
13. DeNardo, D.G., and Ruffell, B. (2019). Macrophages as regulators of tumor immunity and immunotherapy. Nat. Rev. Immunol. *19*, 369–382.
14. Bortolomeazzi, M., Keddar, M.R., Montorsi, L., Acha-Sagredo, A., Benedetti, L., Temelkovski, D., Choi, S., Petrov, N., Todd, K., Wai, P., et al. (2021). Immunogenomics of colorectal cancer response to checkpoint blockade: analysis of the KEYNOTE 177 trial and validation cohorts. Gastroenterology *161*, 1179–1193.
15. Loeuillard, E., Yang, J., Buckarma, E., Wang, J., Liu, Y., Conboy, C., Pavelko, K.D., Li, Y., O'Brien, D., Wang, C., et al. (2020). Targeting tumor-associated macrophages and granulocytic myeloid-derived suppressor cells augments PD-1 blockade in cholangiocarcinoma. J. Clin. Invest. *130*, 5380–5396.
16. Ringelhan, M., Pfister, D., O'Connor, T., Pikarsky, E., and Heikenwalder, M. (2018). The immunology of hepatocellular carcinoma. Nat. Immunol. *19*, 222–232.
17. Sia, D., Jiao, Y., Martinez-Quetglas, I., Kuchuk, O., Villacorta-Martin, C., Castro de Moura, M., Putra, J., Camprecios, G., Bassaganyas, L., Akers, N., et al. (2017). Identification of an immune-specific class of hepatocellular carcinoma, based on molecular features. Gastroenterology *153*, 812–826.
18. Garner, H., and de Visser, K.E. (2020). Immune crosstalk in cancer progression and metastatic spread: a complex conversation. Nat. Rev. Immunol. *20*, 483–497.
19. Gentles, A.J., Newman, A.M., Liu, C.L., Bratman, S.V., Feng, W., Kim, D., Nair, V.S., Xu, Y., Khuong, A., Hoang, C.D., et al. (2015). The prognostic landscape of genes and infiltrating immune cells across human cancers. Nat. Med. *21*, 938–945.
20. Qiu, L., Meng, Y., Wang, L., Gunewardena, S., Liu, S., Han, J., and Krieg, A.J. (2021). Histone lysine demethylase 4B regulates general and unique gene expression signatures in hypoxic cancer cells. MedComm *2*, 414–429.
21. Song, Y., Wu, F., and Wu, J. (2016). Targeting histone methylation for cancer therapy: enzymes, inhibitors, biological activity and perspectives. J. Hematol. Oncol. *9*, 49.
22. Sarno, F., Nebbioso, A., and Altucci, L. (2020). DOT1L: a key target in normal chromatin remodelling and in mixed-lineage leukaemia treatment. Epigenetics *15*, 439–453.
23. Curran, E.K., Godfrey, J., and Kline, J. (2017). Mechanisms of immune tolerance in leukemia and lymphoma. Trends Immunol. *38*, 513–525.
24. Hegde, P.S., and Chen, D.S. (2020). Top 10 challenges in cancer immunotherapy. Immunity *52*, 17–35.
25. Bejarano, L., Jordão, M.J.C., and Joyce, J.A. (2021). Therapeutic targeting of the tumor microenvironment. Cancer Discov. *11*, 933–959.
26. Hiam-Galvez, K.J., Allen, B.M., and Spitzer, M.H. (2021). Systemic immunity in cancer. Nat. Rev. Cancer *21*, 345–359.
27. Lin, H., Kryczek, I., Li, S., Green, M.D., Ali, A., Hamasha, R., Wei, S., Vatan, L., Szeliga, W., Grove, S., et al. (2021). Stanniocalcin 1 is a phagocytosis checkpoint driving tumor immune resistance. Cancer Cell *39*, 480–493.e6.
28. Li, G., Kryczek, I., Nam, J., Li, X., Li, S., Li, J., Wei, S., Grove, S., Vatan, L., Zhou, J., et al. (2021). LIMIT is an immunogenic lncRNA in cancer immunity and immunotherapy. Nat. Cell Biol. *23*, 526–537.
29. Wei, Y., Lao, X.M., Xiao, X., Wang, X.Y., Wu, Z.J., Zeng, Q.H., Wu, C.Y., Wu, R.Q., Chen, Z.X., Zheng, L., et al. (2019). Plasma cell Polarization to the immunoglobulin G phenotype in hepatocellular carcinomas involves epigenetic alterations and promotes hepatoma progression in mice. Gastroenterology *156*, 1890–1904.e16.
30. Wei, Y., Zhao, Q., Gao, Z., Lao, X.M., Lin, W.M., Chen, D.P., Mu, M., Huang, C.X., Liu, Z.Y., Li, B., et al. (2019). The local immune landscape determines tumor PD-L1 heterogeneity and sensitivity to therapy. J. Clin. Invest. *129*, 3347–3360.

31. Zhou, J., Tang, Z., Gao, S., Li, C., Feng, Y., and Zhou, X. (2020). Tumor-associated macrophages: recent insights and therapies. Front. Oncol. *10*, 188.

32. Xiang, X., Wang, J., Lu, D., and Xu, X. (2021). Targeting tumor-associated macrophages to synergize tumor immunotherapy. Signal Transduct. Target. Ther. *6*, 75.

33. Medrek, C., Pontén, F., Jirström, K., and Leandersson, K. (2012). The presence of tumor associated macrophages in tumor stroma as a prognostic marker for breast cancer patients. BMC Cancer *12*, 306.

34. Tu, D., Dou, J., Wang, M., Zhuang, H., and Zhang, X. (2021). M2 macrophages contribute to cell proliferation and migration of breast cancer. Cell Biol. Int. *45*, 831–838.

35. Wang, Y., Wang, J., Yang, C., Wang, Y., Liu, J., Shi, Z., Chen, Y., Feng, Y., Ma, X., and Qiao, S. (2021). A study of the correlation between M2 macrophages and lymph node metastasis of colorectal carcinoma. World J. Surg. Oncol. *19*, 91.

36. Byun, W.S., Kim, W.K., Han, H.J., Chung, H.J., Jang, K., Kim, H.S., Kim, S., Kim, D., Bae, E.S., Park, S., et al. (2019). Targeting histone methyltransferase DOT1L by a novel Psammaplin A analog inhibits growth and metastasis of triple-negative breast cancer. Mol. Ther. Oncolytics *15*, 140–152.

37. Kurani, H., Razavipour, S.F., Harikumar, K.B., Dunworth, M., Ewald, A.J., Nasir, A., Pearson, G., Van Booven, D., Zhou, Z., Azzam, D., et al. (2022). DOT1L is a novel cancer stem cell target for triple-negative breast cancer. Clin. Cancer Res. *28*, 1948–1965.

38. Cho, M.H., Park, J.H., Choi, H.J., Park, M.K., Won, H.Y., Park, Y.J., Lee, C.H., Oh, S.H., Song, Y.S., Kim, H.S., et al. (2015). DOT1L cooperates with the c-Myc-p300 complex to epigenetically derepress CDH1 transcription factors in breast cancer progression. Nat. Commun. *6*, 7821.

39. Liu, C., Yang, Q., Zhu, Q., Lu, X., Li, M., Hou, T., Li, Z., Tang, M., Li, Y., Wang, H., et al. (2020). CBP mediated DOT1L acetylation confers DOT1L stability and promotes cancer metastasis. Theranostics *10*, 1758–1776.

40. Yang, J.Y., Jie, Z., Mathews, A., Zhou, X., Li, Y., Gu, M., Xie, X., Ko, C.J., Cheng, X., Qi, Y., et al. (2020). Intestinal epithelial TBK1 Prevents differentiation of T-helper 17 cells and tumorigenesis in mice. Gastroenterology *159*, 1793–1806.

41. Wilson, A.S., Randall, K.L., Pettitt, J.A., Ellyard, J.I., Blumenthal, A., Enders, A., Quah, B.J., Bopp, T., Parish, C.R., and Brüstle, A. (2022). Neutrophil extracellular traps and their histones promote Th17 cell differentiation directly via TLR2. Nat. Commun. *13*, 528.

42. Ruland, J. (2011). Return to homeostasis: downregulation of NF-kappaB responses. Nat. Immunol. *12*, 709–714.

43. Yu, H., Aravindan, N., Xu, J., and Natarajan, M. (2017). Inter- and intra-cellular mechanism of NF-kB-dependent survival advantage and clonal expansion of radioresistant cancer cells. Cell. Signal. *31*, 105–111.

44. Bhat, K.P.L., Balasubramaniyan, V., Vaillant, B., Ezhilarasan, R., Hummelink, K., Hollingsworth, F., Wani, K., Heathcock, L., James, J.D., Goodman, L.D., et al. (2013). Mesenchymal differentiation mediated by NF-kappaB promotes radiation resistance in glioblastoma. Cancer Cell *24*, 331–346.

45. Zhang, T., Ma, C., Zhang, Z., Zhang, H., and Hu, H. (2021). NF-κB signaling in inflammation and cancer. MedComm *2*, 618–653.

46. Antonangeli, F., Natalini, A., Garassino, M.C., Sica, A., Santoni, A., and Di Rosa, F. (2020). Regulation of PD-L1 expression by NF-κB in cancer. Front. Immunol. *11*, 584626.

47. Barnes, S.E., Wang, Y., Chen, L., Molinero, L.L., Gajewski, T.F., Evaristo, C., and Alegre, M.L. (2015). T cell-NF-κB activation is required for tumor control in vivo. J. Immunother. Cancer *3*, 1.

48. Yang, L., and Lin, P.C. (2017). Mechanisms that drive inflammatory tumor microenvironment, tumor heterogeneity, and metastatic progression. Semin. Cancer Biol. *47*, 185–195.